Journal of Catalysis 279 (2011) 48–65

Contents lists available at ScienceDirect

Journal of Catalysis

journal homepage: www.elsevier.com/locate/jcat

A fundamental study of Pt impregnation of carbon: Adsorption equilibrium and particle synthesis

X. Hao, S. Barnes, J.R. Regalbuto *

Department of Chemical Engineering, University of Illinois, MC 110 810 S Clinton Street, Chicago, IL 60607 7000, USA

ARTICLE INFO

Article history:
Received 29 December 2010
Revised 30 December 2010
Accepted 31 December 2010

Keywords:
Catalyst preparation
Pt
Carbon
Strong electrostatic adsorption
$H_2[PtCl_6]$
$[Pt(NH_3)_4]Cl_2$
pH buffering
Wet impregnation
Dry impregnation

ABSTRACT

To determine whether the method of "strong electrostatic adsorption" (SEA) can be extended to the preparation of carbon-supported Pt catalysts, a series of carbons of different type (activated, black, and graphitic) with different surface areas and points of zero charge (PZC) has been studied. Cationic Pt tetraammine, $[(NH_3)_4Pt]^{2+}$, was adsorbed over low- and mid-PZC carbons in the high pH range, while anionic hexachloroplatinate (IV), $[PtCl_6]^{2-}$, was adsorbed over high-PZC carbons in the low pH range. Adsorption equilibrium was determined by measuring pH and metal concentration in the impregnation solution before and after contacting with the carbon supports. Filtered, dried materials were reduced in hydrogen, and the Pt particle size was characterized by Z contrast imaging.

Electrostatic adsorption occurs at short contact time (1 h) for both Pt anions and cations. The adsorptive behavior of all carbons of like PZC is the essentially the same, independent of type and surface area. There are pH optima at which electrostatic adsorption is strongest; a sharp maximum occurs for anions in the low pH range at pH 2.9, while the high pH optimum for cations is pH 12. To attain the required final values, pH buffering by the surface, a phenomenon not sufficiently appreciated in the literature, has to be overcome. Particles synthesized by SEA are normally in the 1–2 nm range and are as small as or smaller with narrower size distributions than by other methods, especially at high metal loadings.

Results also reveal a longer time scale, reductive mechanism that occurs with Pt(IV) chlorides over carbon at low pH, which mitigates the need for precise pH control if the contact time is long, and might explain the small particle sizes obtained by dry impregnation with the $[PtCl_6]^{2-}$ complex. This mechanism will be more fully explored in future work.

1. Introduction

In efforts to help turn the art of catalyst preparation into science, we have developed the method of "Strong Electrostatic Adsorption" (SEA) as a simple, rational approach to synthesize highly dispersed supported metal catalysts [1,2]. The method is based on an electrostatic mechanism [3] in which the (typically hydroxyl) functional groups on the support surface can be protonated and deprotonated and so positively or negatively charged as a function of pH relative to the point of zero charge (PZC). At the pH of strongest interaction, oppositely charged metal coordination complexes adsorb in a well-dispersed monolayer, and the high dispersion of the precursor phase is retained as the precursor is reduced to metal. To date, the electrostatic mechanism has been demonstrated for noble and base metal coordination complexes, including anionic Pt chlorides (and related hydrolysis complexes) over alumina at low pH [4], and at high pH, cationic Pt tetraammines over silica [5,6] and other noble and base metal ammines over amorphous [7] and mesoporous [8] silicas. Electrostatic adsorption was suggested to be the reason for Pt and Cu overexchange in low Al zeolites [9].

The various forms of carbon (activated, blacks, and graphite) comprise a versatile set of support materials especially for robust operation in liquid phase reactions such as hydrogenations in the pharmaceutical industry or new applications in the conversion of carbohydrates to hydrocarbon biofuels [10,11].

Numerous publications suggest that an electrostatic mechanism plays a role in the adsorption of metal coordination complexes with carbon surfaces, starting with the electrostatic "equilibrium adsorption" studies of molybdate uptake onto carbons of various PZCs [12]. Unoxidized black and activated carbons have PZCs around 9. Unoxidized carbon surfaces contain little oxygen groups but can become positively charged by protonation of the pi bonds in aromatic rings [13,14]. Introducing oxygen functional groups through various liquid or gas phase treatments lowers the PZC by a few to many pH units. Low PZC surfaces have functional groups such as carboxylic acids that deprotonate and become negatively charged at pH values above their PZC.

* Corresponding author. Fax: +1 312 996 0808.
E-mail address: jrr@uic.edu (J.R. Regalbuto).

0021-9517/$ - see front matter © 2011 Published by Elsevier Inc.
doi:10.1016/j.jcat.2010.12.021

Untreated graphitic carbons have mid- to low PZCs [12,14,15]. By altering the PZC of carbons in a systematic manner, the adsorptive properties of carbon surfaces might be controlled [14,15].

In a comprehensive review in 1997 by Radovic and Rodriguez-Reinoso, electrostatic adsorption is presented as the centerpiece of carbon catalyst preparation [14]. Consistent with electrostatic adsorption, several studies indicate that less severe oxidation (and correspondingly higher PZCs) leads to greater uptake of hexachloroplatinate (IV) anions ($[PtCl_6]^{2-}$, commonly referred to as chloroplatinic acid, or CPA) [16–19]. Heat-treated carbon, presumably with less surface oxygen and higher PZCs, adsorbs more CPA than oxidized carbon [16,20]. Chloroplatinate adsorption isotherms indicated that the interactions of the metallic precursor with the carbon surface were higher for carbons of low acidity (and presumably higher PZC) [21]. Surface oxygen groups, which lower PZC, have been reported to favor the anchoring of cationic platinum tetraammine ($[(NH_3)_4Pt]^{2+}$, or PTA) [14,22].

On the other hand, even after Radovic and Rodriguez-Reinoso's comprehensive review, it has been reported that increasing oxygen groups on the carbon surface had no effect on PTA uptake [23,24] or CPA uptake [24,25]. In other reports, increasing surface O yielded higher dispersion with CPA [16,27]. In yet other work, surface oxidation had a negative effect on dispersion using PTA [28,29]. Numerous authors have cited a reactive interaction of CPA with carbon [16,18,21,23,25,30,31]. There still does not appear to be a general consensus of the electrostatic or other mechanisms by which common Pt precursors interact with carbon surfaces. That common understanding is the goal of this study.

Results from our preliminary investigation over activated carbons are reproduced in Fig. 1[15]. The qualitative trends of electrostatic adsorption are indeed seen; the carbon with the highest PZC (unoxidized) adsorbs the most anions (Fig. 1a). That with the lowest PZC adsorbs the most cations (Fig. 1b). A carbon with an intermediate PZC displays intermediate uptake in each regime. In both pH regimes, the uptake – pH curves are volcano-shaped, which is a further indication of electrostatic adsorption [3].

However, there are several notable quantitative differences from a purely electrostatic model. The trends of CPA and PTA uptake over surfaces of different PZC from the "Revised Physical Adsorption" (RPA) model [3] are shown in Fig. 1c. Since ammine complexes adsorb with two hydration sheaths intact, instead of one for the anions [32], the cationic uptake is inherently about half that of the anions. In each pH regime, the curves as a function of PZC are regularly spaced volcano-type curves in which adsorption increases as pH moves away from the PZC and the surface charge builds up, but decreases at pH extremes as high ionic strength decreases the adsorption equilibrium constant [3]. In the low pH regime, a PZC 2.5 (Fig. 1b) carbon adsorbs CPA, whereas the RPA model predicts it should not. In the upper pH regime, the maximum uptake of all three carbons is only about half that anticipated from the RPA model [3].

Using the electrostatic mechanism as a benchmark, this paper presents a systematic study of the mechanism of Pt uptake over a variety of carbons (activated, blacks, and graphites) with a variety of PZCs, in an attempt to discern between electrostatic and reactive components of the metal complex–carbon surface interaction and

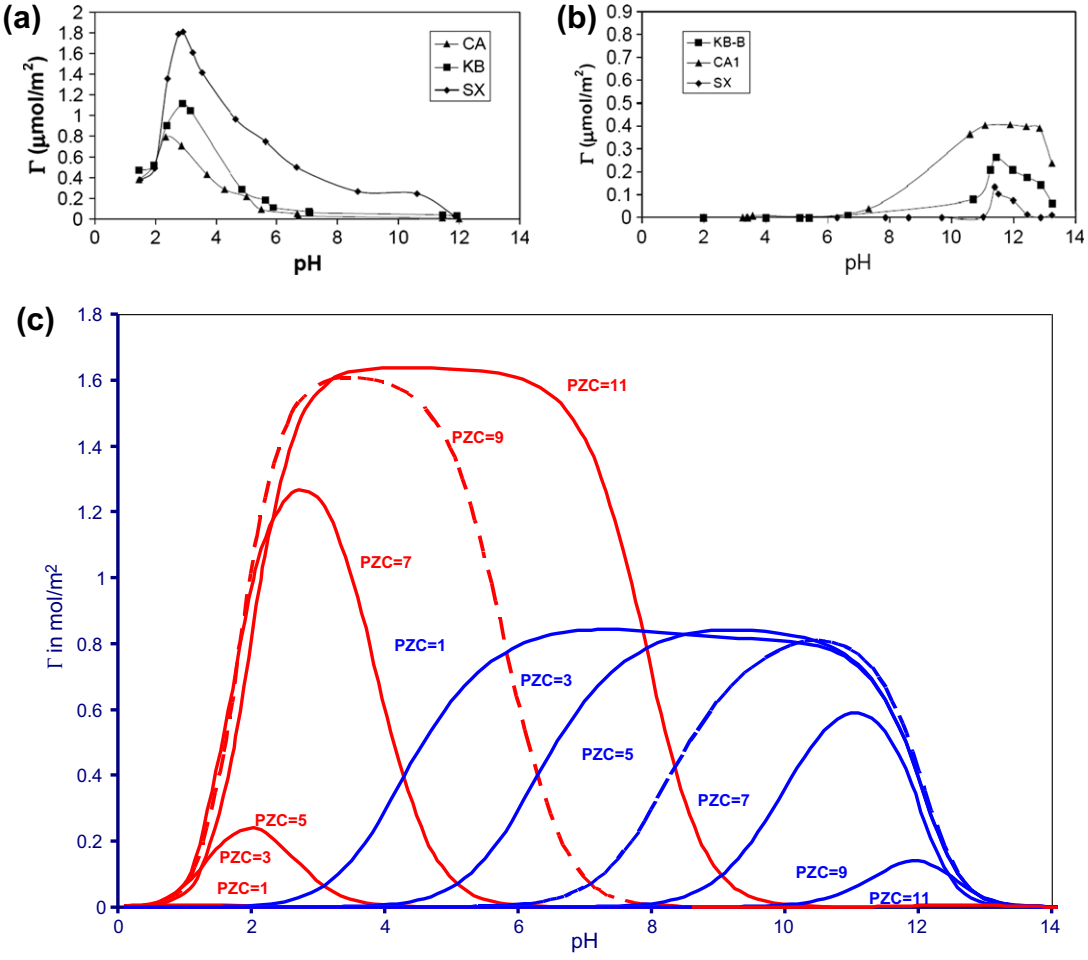

Fig. 1. Pt uptake over carbons of various PZCs versus final pH (500 m^2/L and 200 ppm CPA or 1000 m^2/L and 200 ppm PTA: (a) CPA experimental results, (b) PTA experimental results, and (c) Simulation of uptake of CPA (lower pH range) or PTA (higher pH range) versus pH for various PZC materials (Δpk 4, various PZC, N_S = 5 OH/nm^2).

to provide practical guidance for metal particle synthesis based on this knowledge. Equilibrium studies of Pt anion and cation adsorption and subsequent particle synthesis are given in the present work. Future works will contain XAS and XPS characterization for the molecular characterization of the Pt–carbon interaction and the extension of SEA to high surface area carbon blacks which have potential as fuel cell electrocatalysts and other applications. The method has already been extended to novel mesoporous carbon xerogels for benzene hydrogenation [33] and fuel cell reactions [34].

2. Experimental

2.1. Materials and methods

Six high-purity activated carbons (CA, KB, SXU, SX2, SX4, S51) from Norit America Inc., two high surface area graphite (Asbury, Timrex), and five carbon blacks (VXC, E250, E350, PA, PU) of widely varying surface areas (45–1475 m^2/g) have been selected for this study. The characteristics of carbons are summarized in Table 1. For the sake of comparison, a gamma alumina powder (LaRouche, 277 m^2/g) and a fumed silica (Degussa Aerosil 300, 330 m^2/g) were used. Hexachloroplatinnic acid (H_2PtCl_6) and platinum(II) tetraammine chloride were the main sources of the anionic and cationic species employed and were purchased from Aldrich. For the sake of comparison, sodium tetrachloroplatinate(II), also purchased from Aldrich, was used in one series of experiments.

The PZC of each sample was measured with a simplified version of the pH shift method [35]. Because the plateau is very wide for this technique, 3-point pH shift experiments were applied to get the PZC. Initial pHs were 3.0, 6.0, and 9.0. The results are summarized in Fig. 2. The carbons can be divided into three sections: high PZC (7.5–9), medium PZC (4.8–5.6), and low PZC (2.5) as shown in the plot.

In the adsorption experiments, differences in the specific surface area of each carbon were accounted for by using a constant "surface loading," or in other words, the total support area per liter of solution. A target value is achieved by varying the mass of the particular carbon. For CPA experiments, a value of 500 m^2/L was employed, and to permit a high enough PTA concentration for simple and accurate ICP measurement, 2000 m^2/L was employed for PTA experiments.

Fifty milliliters of dilute CPA, adjusted to various pH values using HCl or NaOH, was added to carbon powders previously weighed into polypropylene bottles. The amount of Pt in solution corresponded to about 10% excess of 1.6 μmol Pt/m^2 for anionic Pt or 0.84 μmol Pt/m^2 for cationic Pt [30]. The bottles were placed on a rotary shaker and intermittently sampled for pH. At 1 or 24 h, 3- to 4-mL portions of the well-mixed suspensions were removed from the bottles and the solid was filtered to permit the measurement of Pt in the liquid phase by ICP. Adsorption density is calculated as the initial minus final concentration of Pt divided by the surface loading and is expressed as micromoles Pt adsorbed per square meter.

The pH of the CPA and PTA solutions needs to be finely adjusted to achieve adsorption surveys with well-distributed final pH values. For CPA, in the pH range in which HCl is needed, the procedure is simple by just adding the difference of the $[H^+]$ concentration between the object pH and the natural pH of CPA, which is 2.43 for 200 ppm Pt. In the pH range in which base is needed, an aging procedure is needed because of the hydrolysis of $[PtCl_6]^{2-}$, which requires several days to equilibrate. A method was developed to arrive at pH values in this range without having to add a great deal of acid or base solution, which minimizes changes in the Pt concentration and the ionic strength. Around five bottles of CPA solutions were prepared with different amounts of base and aged for 48 h. The pH of the mid-pH range solutions can drop from 0.5 to 2 pH unit depending on the pH. Different amounts of NaOH (1 M) are added to get a pH range from 2.7 to 12. Because of the high sensitivity of the pH to the added amount of NaOH, pHs after aging 48 h were often not precisely spaced, and further pH adjustment was needed. To maintain low ionic strength, CPA solutions of different pHs are mixed to obtain a pH in between. For example, if pH 5 is needed, a pH 4 sample can be mixed with a pH 9 sample. After the second pH adjustment, samples were aged for another 42–48 h. Details can be found elsewhere [36]. PTA only needed basification and basified solutions equilibrated in minutes were stable.

2.2. Particle synthesis and characterization

To synthesize sufficient amounts of SEA-prepared material for subsequent characterization, adsorption experiments at the optimal pH (2.9 for CPA and 12 for PTA) were conducted with 250 mL of solution at 500 and 2000 m^2/L, respectively. ICP was used to measure metal uptake and in all cases mirrored the results obtained at the smaller scale. The weight percent of metal on each support is listed in Table 2. The filtered solids were washed and

Table 1
Pertinent properties of carbons.

Carbon name	Abbreviation	Surface area B.E.T (m^2/g)	Pretreatment	Total pore volume (ml/g)	PZC[a]
Activated carbon					
Darco s-51	S51	650	Acid-washed, steam activation of lignite coal	1.0	4.7
Norit SX 2	SX2	800	Acid-washed steam-activated	1.36	8.4
Norit SX 4	SX4	650	Acid-washed steam-activated		7.9
Norit SX ULTRA	SXU	1200	Acid-washed steam-activated	2.16	7.8
Norit CA-1	CA	1400	Chemically activated by phosphoric acid	0.9	2.6
Darco KB-B	KB	1500	Chemical activation of hardwood	1.8	4.8
Graphite					
Asbury Grade 4827	ASBURY	115	Heated, ground natural graphite	2.55	5.2
Timcal TIMREX HSAG 300	TIMREX	280	Heated, ground petroleum coke	1.64	4.5
Carbon black					
Ensaco 250 Powder	E250	62	Pyrolysis	1.4	9.0
Black Pearls 2000	BP2000	1475	Pyrolysis	7.2	9.5
Ketjen 300	K300	795	Pyrolysis	7.0	9.4
Printex A	PA	45	Pyrolysis	2.5	9.4
Printex U	PU	100	Pyrolysis	4.6	5.3
Ensaco 350 Powder	E350	770	Pyrolysis	8.0	9.5
Vulcan XC 72	VXC	254	Pyrolysis	3.46	8.9

[*] Determined by pH shift method of [35].

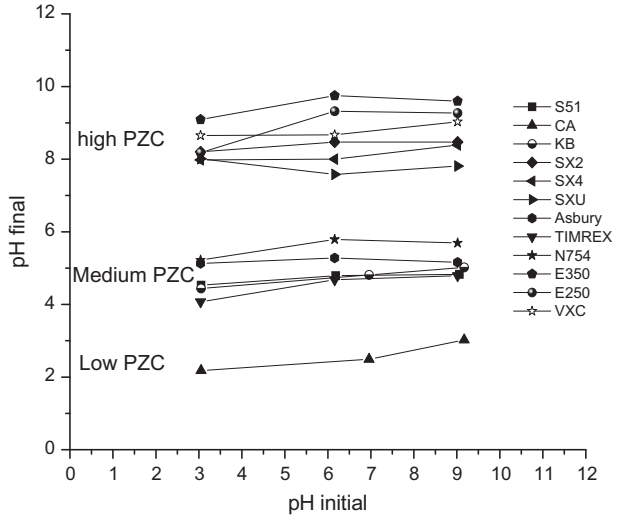

Fig. 2. pH shift results for various carbons.

dried at ambient temperature for 48 h and then placed in an oven at 100 °C for 12 h.

For the sake of comparison, the same weight percent Pt catalysts were prepared by incipient wetness (or dry impregnation, DI) using CPA, PTA, and Na_2PtCl_4. An appropriate amount of either CPA or PTA was dissolved in corresponding amounts of deionized water and impregnated into approximately 0.25 g of carbon. For the Pt(II) chloride preparations, the Pt salt was added to a solution acidified with nitric acid to the equivalent to $2H^+$/Pt in order to have the same initial pH as if the solution were made from CPA. For all DI preparations, the drying step was the same as that used for the SEA preparations.

Based on TPR identification of the respective reduction temperatures, dried CPA/carbon was reduced at 160 °C and dried PTA/carbon was reduced (50 sccm pure H_2, 1 h) at 200 °C prior to scanning transmission electron microscopy (STEM) analysis. For comparison with the literature, a few PTA samples were reduced at 400 °C. High-angle annular dark field (HAADF) imaging was performed using a JEM-2010F electron microscope. Particle size analysis was performed typically using 500–1000 particles obtained from 4–6 representative regions of the material, using the image analysis program Particle2 provided by Dr. Catherine Louis at Universite Pierre et Marie Curie.

3. Results

3.1. pH shift control experiments

To demonstrate the dramatic effect that carbon surfaces can have on solution pH and to compare carbons with typical oxide supports, plots of final pH versus initial pH are shown in Fig. 3 (these are expanded versions of Fig. 2) for various surface loadings of carbon and oxides. Fig. 3a is for Vulcan XC 72, a typical high-PZC carbon, at 6000, 60,000, and 106,000 m^2/L, the latter value of which corresponds to dry impregnation (at 2.4 mL/g). Even at the low surface loading, which corresponds to 1 g of 250 m^2/g carbon in 40 mL, the pH can shift upward over 2 pH units in the acidic regime as protons are taken up by the carbon surface. Comparing the carbon pH shifts to those of alumina at the same surface loading, it is seen that the alumina plateau is about 2–3 pH units wider than that of carbon. Furthermore, where the alumina plot shows substantial displacement from the diagonal in the basic pH regime, that for carbon does not deviate nearly as much; there is much more deprotonation from the alumina surface at high pH than from the carbon surface.

Similar pH shift plots for Timrex, a typical mid-PZC carbon, are shown in Fig. 3b and can be compared with silica. Large pH shifts are seen even for the lower surface loading of carbon. The width of the 60,000 m^2/L carbon pH plateau is somewhat wider than that of silica in the upper pH regime. Dry impregnation (at 1.25 mL/g) gives a surface loading of 224,000 m^2/L.

In part c of Fig. 3, the pH shifts of high-, mid-, and low-PZC carbons are shown at surface loadings of 500, 2000, and 2000 m^2/L, respectively, which mirror the values to be used in Pt adsorption experiments. Data are shown for one and 24 h of contact; there is no appreciable difference between the two times.

3.2. CPA adsorption over carbon

A first set of adsorption experiments consisted of monitoring Pt uptake and shifts in pH after CPA was added at constant

Table 2
STEM particle size distribution of various carbon supports.

Sample	SA (m^2/g)	PZC	wt% Pt	DI		SEA	
				Ave. diam. (nm)	Std. dev. (nm)	Ave. diam. (nm)	Std. dev. (nm)
CPA/high PZC							
Activated carbons							
SXU	1200	8.1	13.5	2.4	0.5	1.9	0.7
SX2	800	8.4	12.0	2.1	0.4	2.8	0.9
Carbon blacks							
PA	45	9.4	1.3	1.5	0.4	2.3	0.8
E250	62	9.0	2.0	1.9	0.6	2.3	0.6
Vul	254	8.9	10.0	2.5	0.7	1.5	0.6
K300	795	9.4	17.9	2.3	0.5	2.6	0.8
BP2000	1475	9.5	28.0	2.3	0.6	2.0	0.7
PTA/mid-PZC							
Activated carbons							
s-51	650	4.7	2.0	3.1	0.9	1.4	0.3
KB-B	1500	4.8	5.3	V. large	NA	2.0	0.5
Carbon blacks							
PU	100	5.3	0.5	2.6	1.3	1.8	0.4
Graphitic carbons							
Asb	115	5.2	1.1	1.6	0.5	1.1	0.3
Tim	280	4.5	2.3	1.5	0.7	1.2	0.3

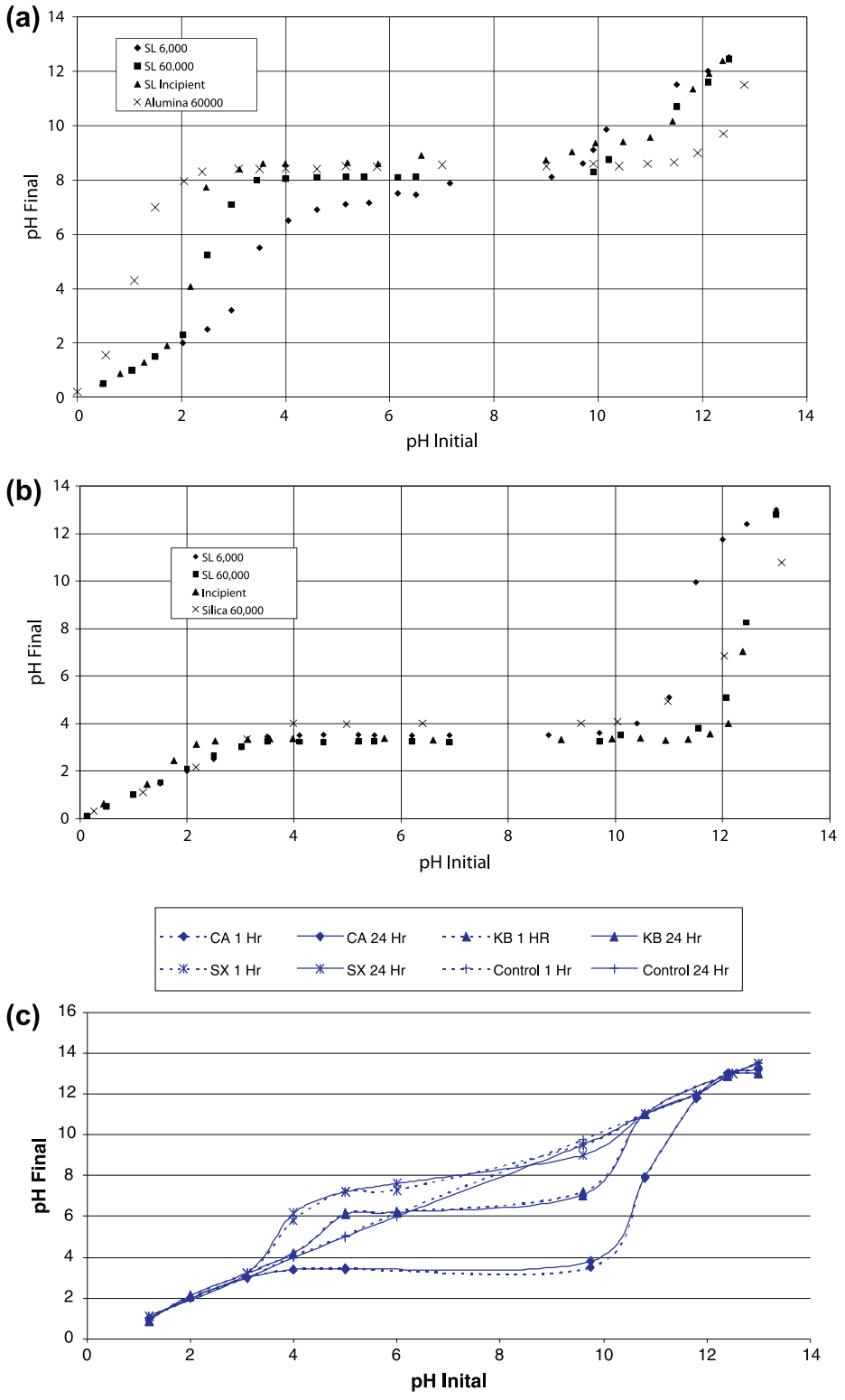

Fig. 3. pH shift comparisons of carbons with oxides of similar PZC: (a) Vulcan XC72 with gamma alumina, (b) Timrex graphitic carbon with fumed silica, (c) pH shifts at 1 and 24 h.

concentration to various carbons at different initial pH values. The Pt concentration of 180 ppm (9.2×10^{-4} M) corresponds to about a 10% excess of one monolayer of Pt (1.6 μmol/m^2) for the employed surface loading of 500 m^2/L. Platinum uptake (in μmol/m^2) on the high-PZC range carbons at 1 h and 24 h is summarized in Fig. 4.

At both 1 h (Fig. 4a) and 24 h (Fig. 4b), the uptake of Pt is similar for all carbon samples and shows a volcano-shaped curve with maximum at about 2.9. This volcano-type curve has been seen previously for CPA adsorption over alumina [4] and in our previous study of carbon [15]. The six carbon samples differ in type (SX4, SX2, SXU are activated carbon, and VXU, E250, E350 are carbon

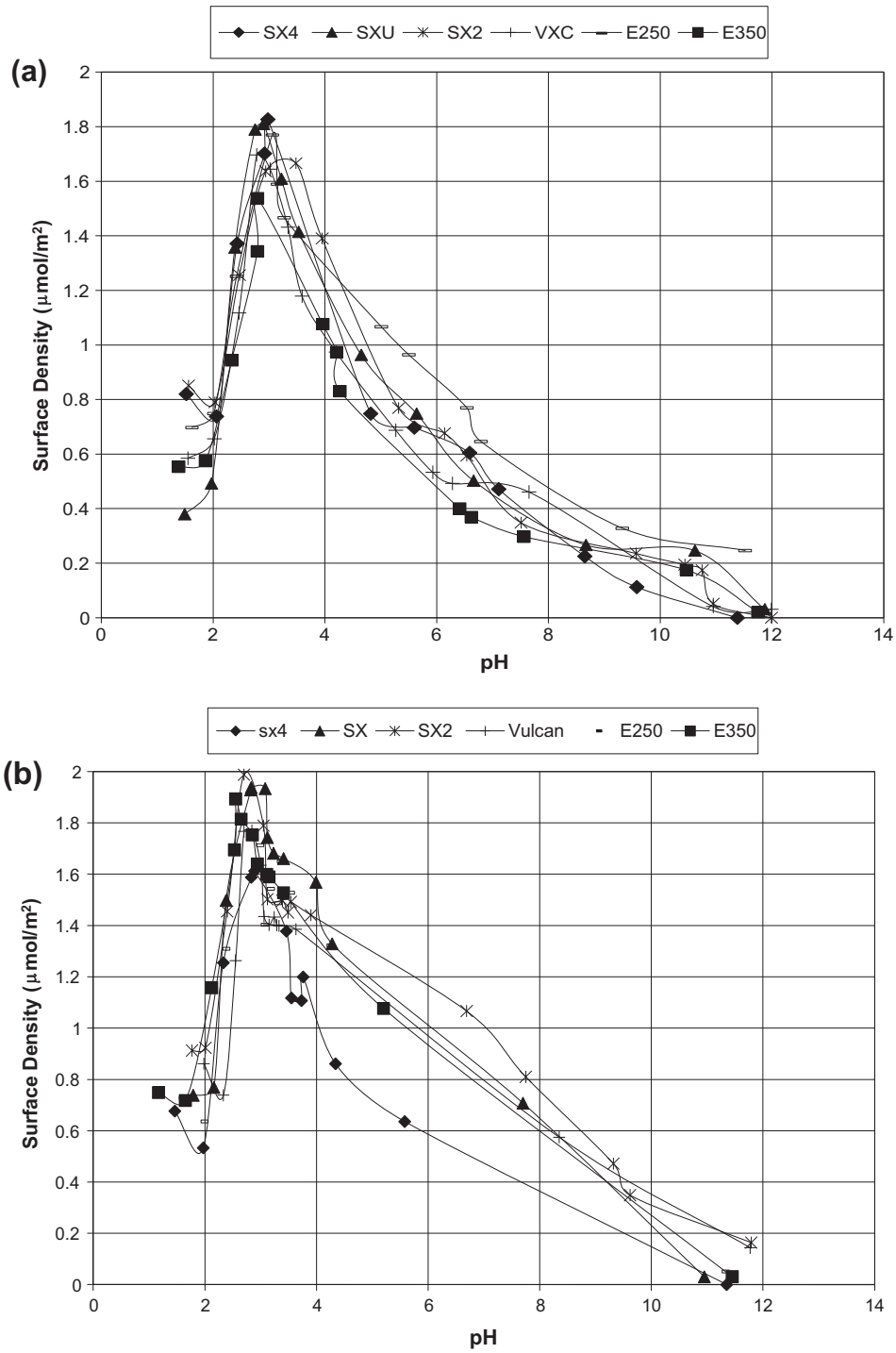

Fig. 4. Pt uptakes over high-PZC carbons versus pH at (a) 1 h and (b) 24 h. Pt uptake over medium-PZC carbons versus pH at (c) 1 h and (d) 24 h. Pt uptakes over low-PZC carbon versus pH at (e) 1 h and (f) 24 h.

black) and surface area (from 62 m^2/g for E250 to 1200 m^2/g for SXU). It appears that CPA has access to all pores of even the high surface area materials, since the maximum uptake is about the same for these as for lower surface area materials with larger pores. Small differences in the maximum uptake may arise from inaccuracies in the BET surface area measurements. A key feature of this overlapping data set is that the differences in specific surface area were accounted for by employing a constant surface loading.

Subtle differences are observed between the short and long contact times. First, the maximum uptake has increased by about 10%, and second, there is a general shift in data points from the mid-pH regime to lower pH at long contact times, which causes the data points to "climb" the slope of the volcano as the pHs drop by aging. The lowest pH values do not shift appreciably.

Fig. 4c and d shows the Pt uptake on carbon samples in the mid-PZC range around 5. Once again, the uptake curves for all carbons are similar; the maximum uptake is around a pH of 2.9 and the Pt surface densities are almost the same for all mid-PZC carbons but are somewhat lower than for the high-PZC carbons. This trend was reported for a single series of activated carbons in our earlier

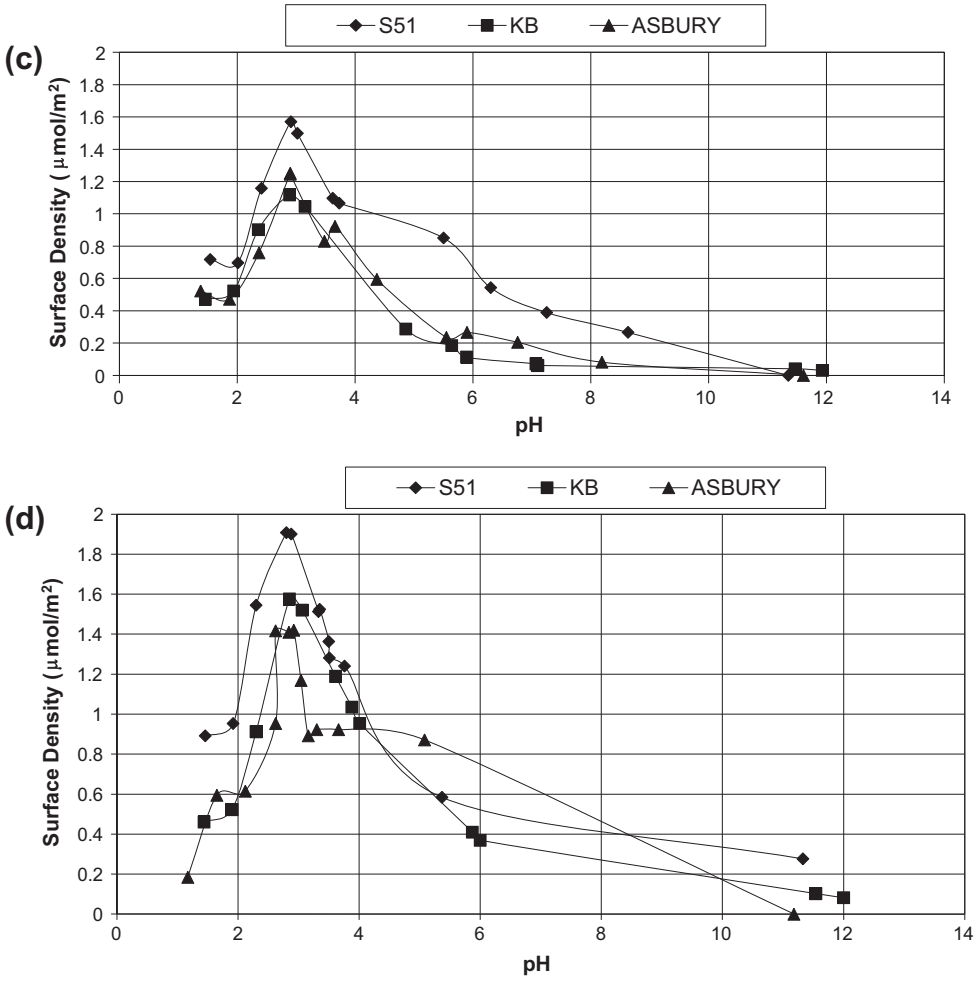

Fig. 4 (*continued*)

work [15]. As occurred for the high-PZC carbons of Fig. 4a and b, maximum uptake increases with the long exposure time and the mid-pH range data points drift down in pH and up the adsorption volcano. For both times, the amount of Pt adsorbed on carbon surface is larger than what the RPA model predicts for a simple oxide PZC near 5 (Fig. 1a).

The uptake of CPA over the low-PZC carbon, CA, is shown in Fig. 4e and f. There is an appreciable difference between the uptake at 1 h and 24 h. Once more the maximum surface density of Pt increased from 0.8 to 1.3 μmol/m^2 as the pH values in the central pH regime drift downward. Comparing the high-, medium-, and low-PZC carbon samples, it appears that the lower the PZC, the higher the increase of the Pt uptake from 1 to 24 h.

The shifts in pH that occurred during adsorption at 1 and 24 h are shown in Fig. 5. Recall that in the control experiments without Pt in solution, Fig. 3c, there is no appreciable pH shift between 1 and 24 h. On the other hand, in Fig. 5a for the high-PZC carbons, the 1-h pH values are close to the 1-h control values, while the 24-h values have shifted considerably down, forming a plateau near pH 3–3.5. The 24-h pH shifts for the mid-PZC set of carbons in Fig. 5b are similar. In all cases but KB, the 24-h pH values have shifted considerably down from the 1-h values, in contrast to the Pt-free control experiment (Fig. 3c). Significant downward pH shifts at long contact time are also evident for the low-PZC CA sample in the presence of CPA (Fig. 5e) but not in the absence of CPA (Fig. 3c).

3.3. PTA adsorption over carbon

A PTA concentration of 312 ppm (1.4×10^{-3} M) corresponds to about a 10% excess of one monolayer of Pt (0.84 μmol/m^2) for a surface loading of 2000 m^2/L. Platinum uptake (in μmol/m^2) on the various PZC range carbons at 1 and 24 h is summarized in Fig. 6.

Several parameters are seen to control the adsorption of Pt cations. First is the PZC of the carbon; in general the lower the PZC, the higher the surface charge and the higher the Pt uptake. As noted in the introduction, however, the highest surface area carbons (those with the smallest pore sizes) show a significant fraction of pore exclusion for the larger-sized PTA complexes. For that reason, only some of the mid-PZC carbons in Fig. 6c and d achieve high uptake, and the uptake of the low-PZC carbon, CA, in Fig. 6e and f, is lower than that of the larger-pore mid-PZC carbons of Fig. 6. In most cases, only small increases in uptake are seen between 1 and 24 h. The slowest samples to equilibrate were the pH 9–10 data points over the Timrex carbon.

Fig. 7 summarizes the pH shift of the solution when PTA is contacted with carbon. When the pH of the solution is higher than PZC of carbon, the pH will shift down; when pH of the solution is lower than PZC of carbon, the pH will shift up. There is little difference between the 1- and 24-h data for adsorption over all carbons, independent of PZC. Furthermore, comparing the pH shifts with and without Pt tetraammine (Fig. 8), the difference is negligible.

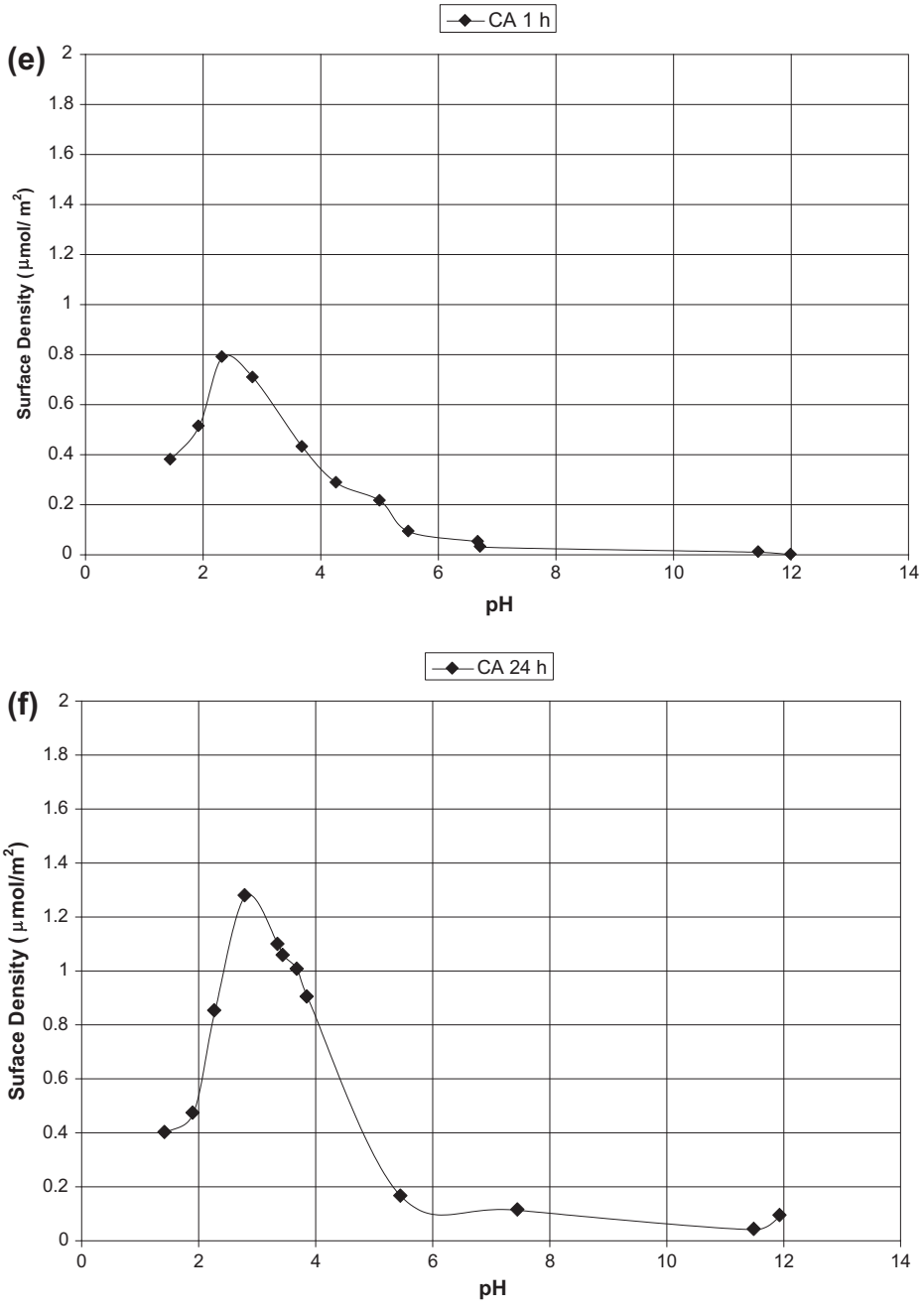

Fig. 4 (*continued*)

3.4. Catalyst synthesis and characterization

Representative STEM images of SEA and DI-prepared CPA/C materials are shown in Fig. 9 and those for SEA and DI-prepared PTA/C in Fig. 10. The mean particle size and standard deviations for each sample are summarized in Table 2. The SEA-prepared PTA samples all show smaller average sizes (1.1–2.0 nm) and tighter standard deviations (about 25% of particle size) than their DI counterparts. The reduction temperature employed for the materials shown in Fig. 10 was 200 °C and the (slow) heating rate was 2 °C/min; however, a PU and an Asbury sample reduced at 400 °C with the same heating rate gave virtually the same particle size and standard deviation. With a higher heating rate of 5 °C/min to 200 °C, the particle sizes were roughly 30% larger for selected samples (PU and Asbury) tested. Interestingly, the particle size range of CPA materials prepared with SEA and DI was roughly the same and was between 1.5 and 2.5 nm and standard deviations of the two sets are similar. Even smaller particles, in the range 1.1–1.3 nm, were synthesized over carbon xerogels at lower metal loading using either SEA or DI with CPA in a previous publication [33].

To contrast the synthesis of materials made from Pt(II) chloride, DI samples were also prepared with this complex over SXU and Vulcan supports. The solutions employed were pH-adjusted with nitric acid ($2H^+$/Pt) to the same value as the corresponding CPA solutions; the only differences in the Pt(IV) (CPA) and Pt (II) DI preparations were the valence of the metal precursor and their geometries (hexachloroplatinate (IV) being octahedral and tetrachloroplatinate (II) being square planar). Representative STEM images are shown in Fig. 11; unlike CPA DI, the particles formed from Pt(II) in both cases were very large and irregularly shaped.

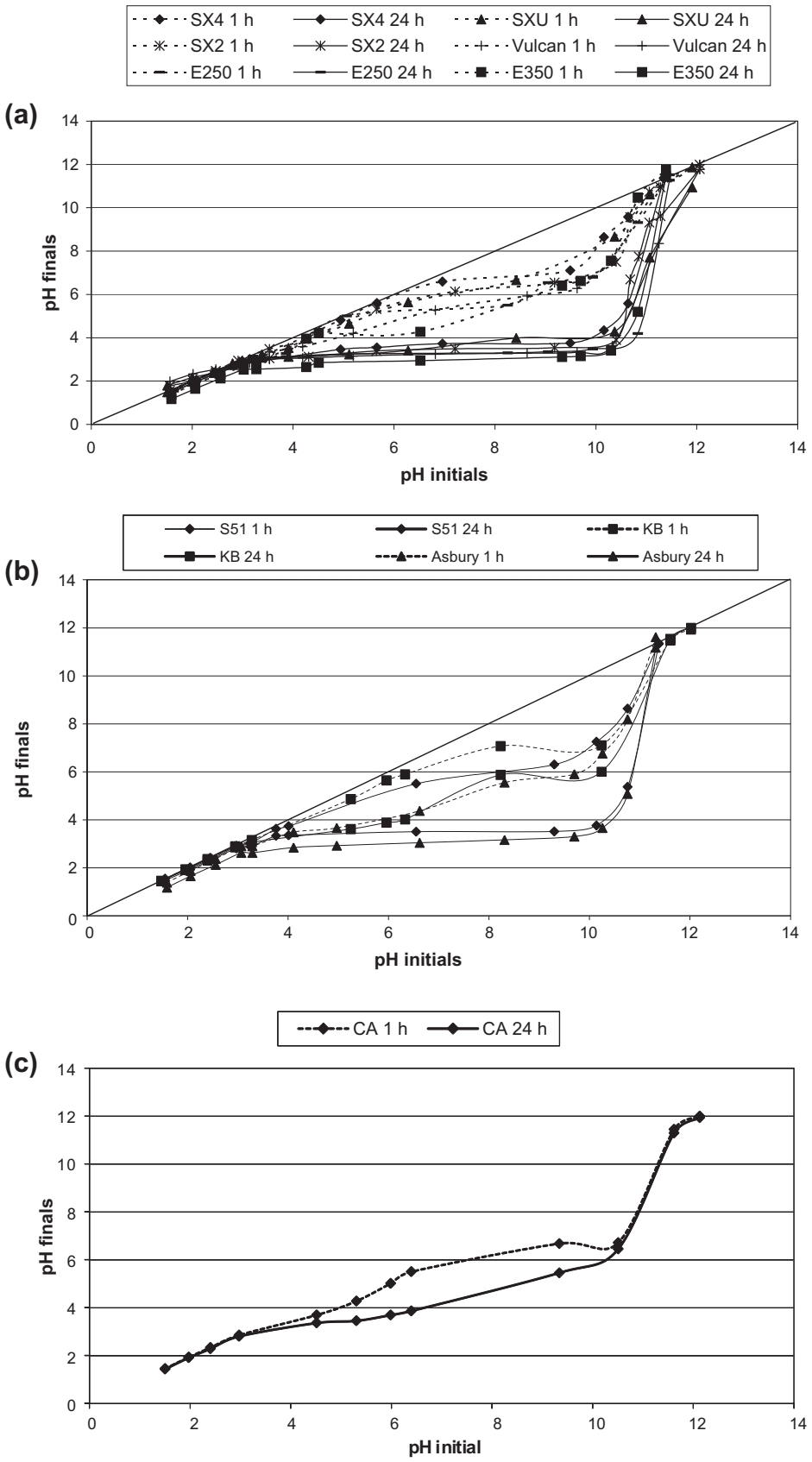

Fig. 5. pH final versus pH initial at 1 and 24 h of contact for (a) high-PZC range, with CPA, (b) medium-PZC range, with CPA, and (c) low-PZC range, with CPA.

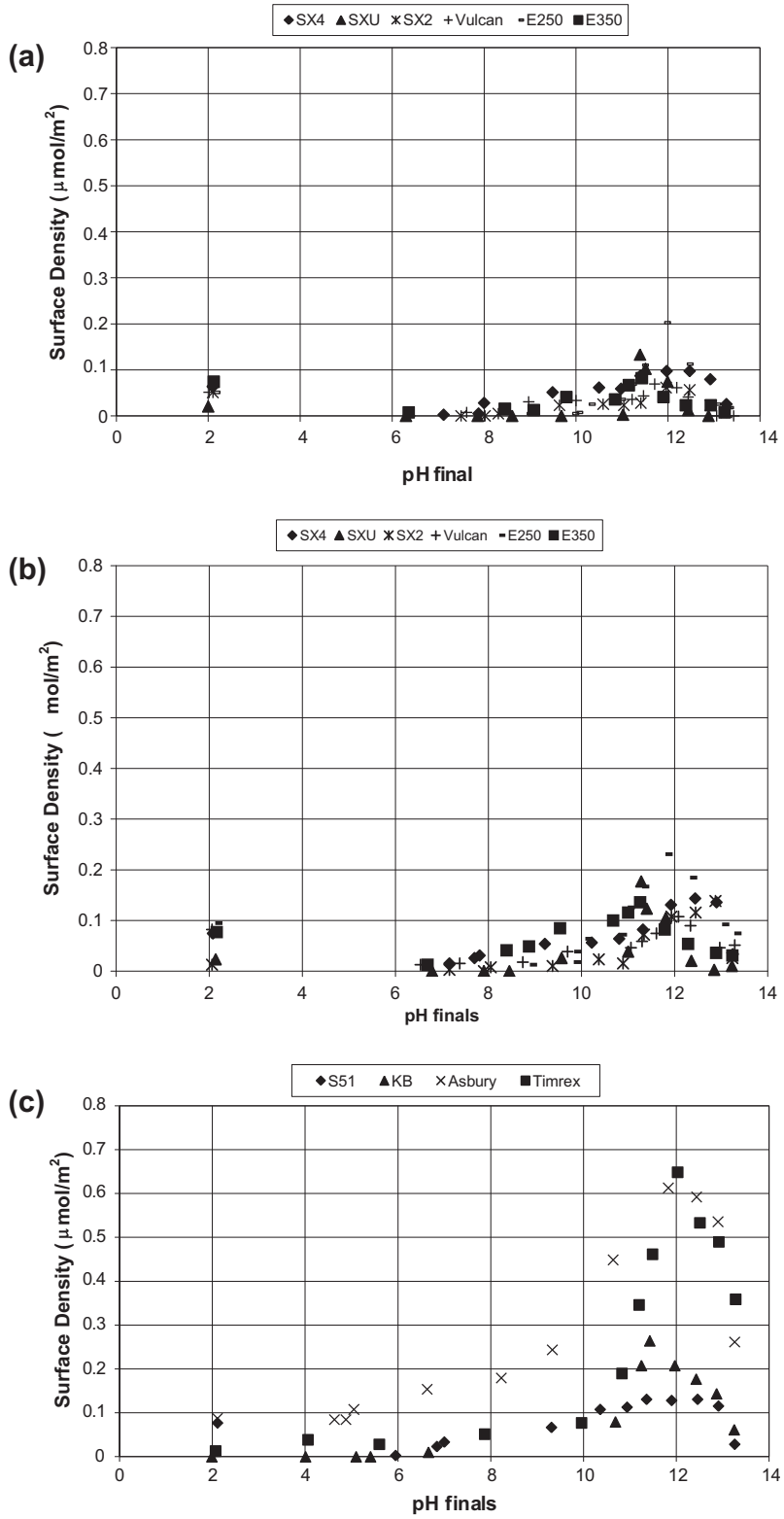

Fig. 6. Pt uptake over high-PZC carbons versus pH at (a) 1 h and (b) 24 h. Pt uptake over medium-PZC carbons versus pH at (c) 1 h and (d) 24 h. Pt uptake over low-PZC carbon versus pH at (e) 1 h and (f) 24 h.

4. Discussion

4.1. Proton transfer to and from the carbon surface

A number of mechanistic details can be inferred from the pH shifts of Fig. 3. First, the high-PZC carbons of Fig. 3a show relatively much greater capacity to adsorb protons below the PZC (deviation from the diagonal in the left-hand side of the plot) than the capacity to give protons up above the PZC (deviation from the diagonal on the right side of the plot). In fact, the high-PZC surfaces have almost no proton-donating capacity. Unlike the amphoteric surface –OH groups on alumina, which can both be protonated at low pH to

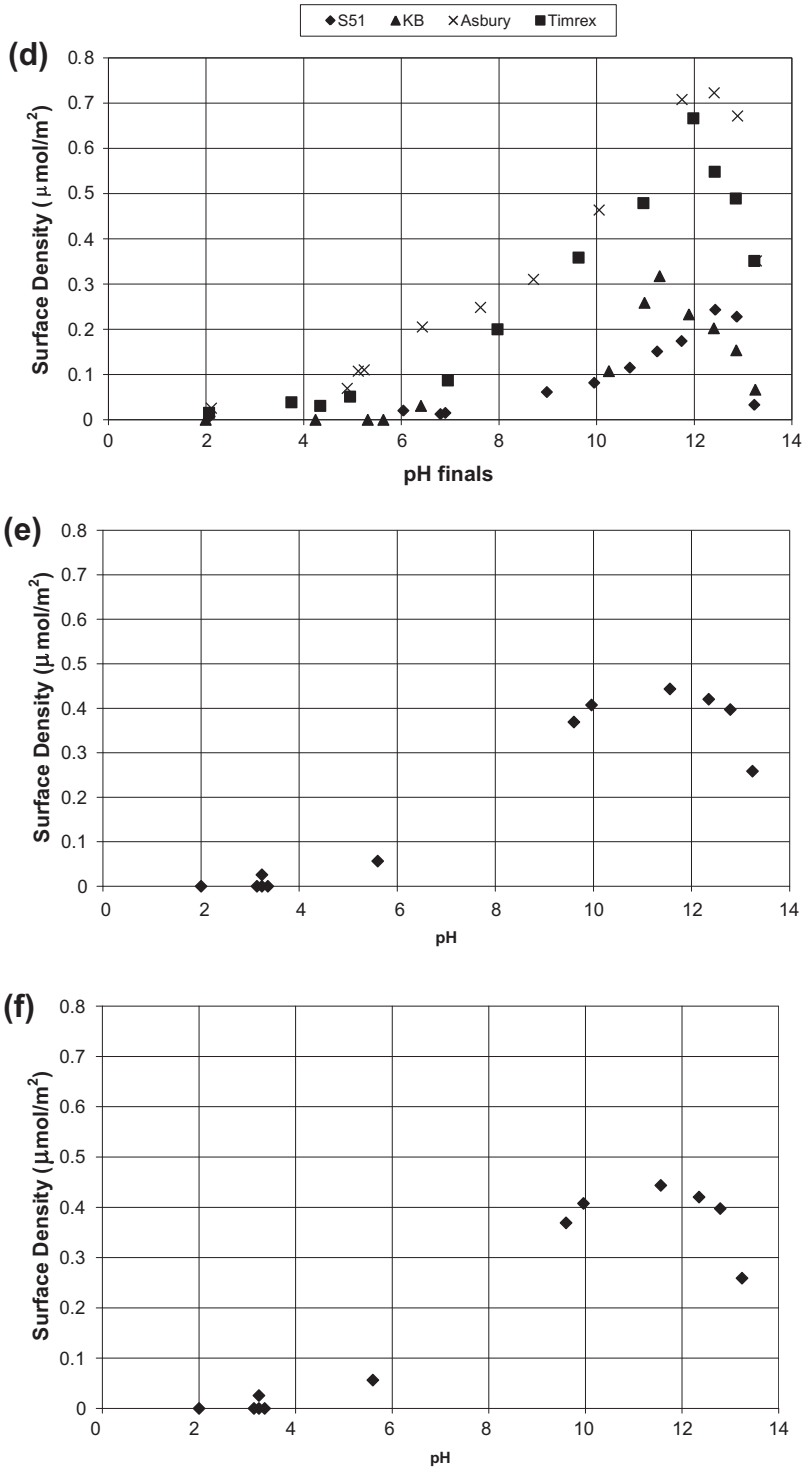

Fig. 6 (*continued*)

form $-OH_2^+$, exist as –OH at the PZC, and deprotonate to $-O^-$ above the PZC, the proton transferring functional groups on the high-PZC carbon are best characterized as single-site, single pK, or monofunctional surface groups. These data support the literature postulation [13,14,16,19] of the one-way protonation of pi bonds of aromatic rings:

$$\pi + H^+ \leftrightarrow \pi - H^+$$

The fact that high-PZC carbons take up relatively very little cationic Pt (Fig. 6a and b) further supports the picture of a single pK surface.

Second, the pH plateau for alumina is over one pH unit wider than that for the high-PZC carbon at the same surface loading (60,000 m^2/L). This indicates that the surface density of protonizable surface groups on this carbon is much less, perhaps over an order of magnitude, than that of the alumina. These data appear consistent with experimental determinations; the –OH density for alumina is typically cited at around 8 OH/nm^2 [3] while titration of high-PZC carbons has been reported in the range 0.005–0.8 meq/g [12,19,37,38], which based on the surface areas of those carbons gives values of 0.014–1.9 groups/nm^2. The smaller density of protonated groups at the carbon surface can explain the

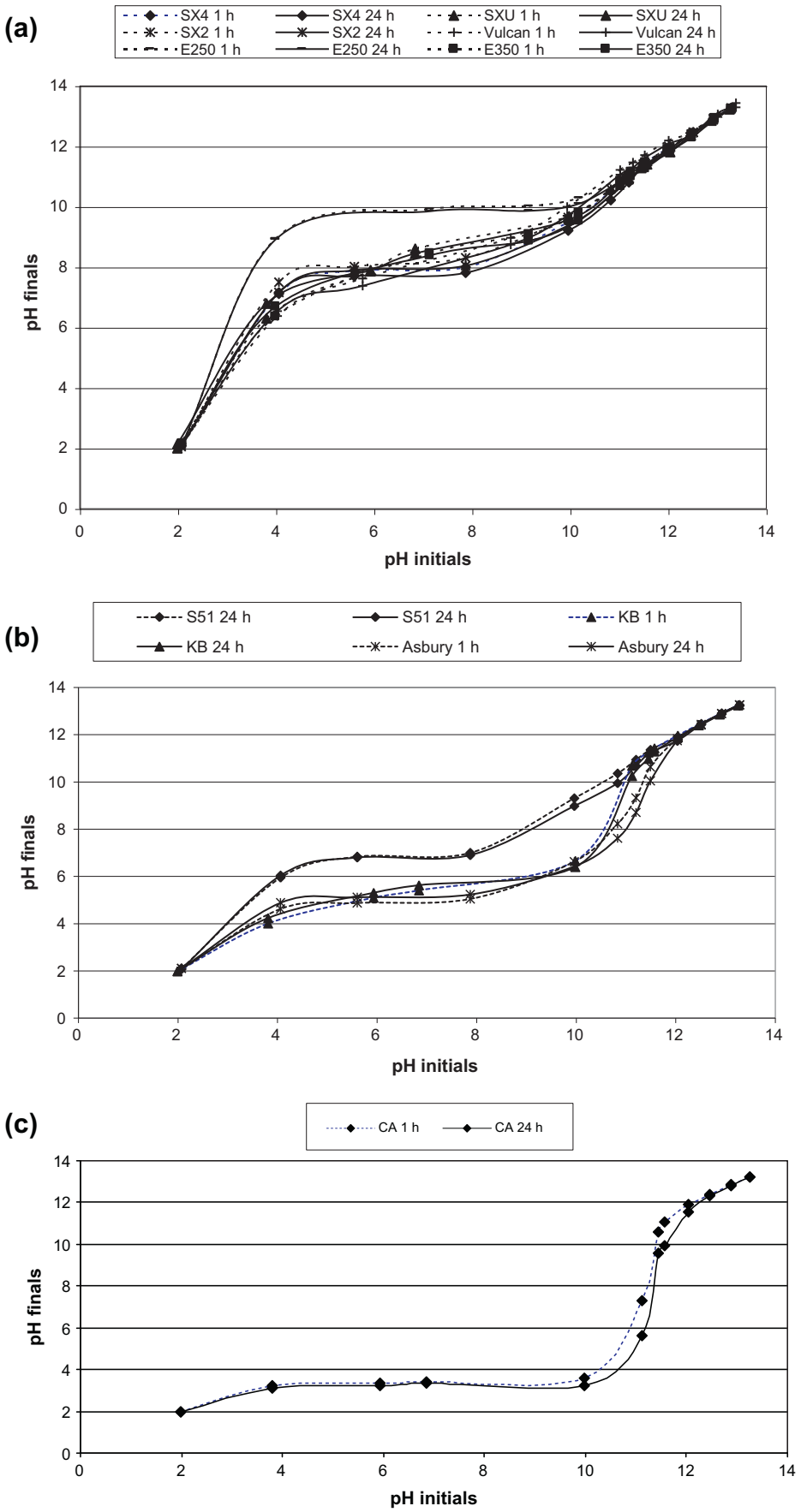

Fig. 7. pH final versus pH initial during PTA adsorption for (a) high-PZC range, (b) medium-PZC range, and (c) low-PZC range carbon samples.

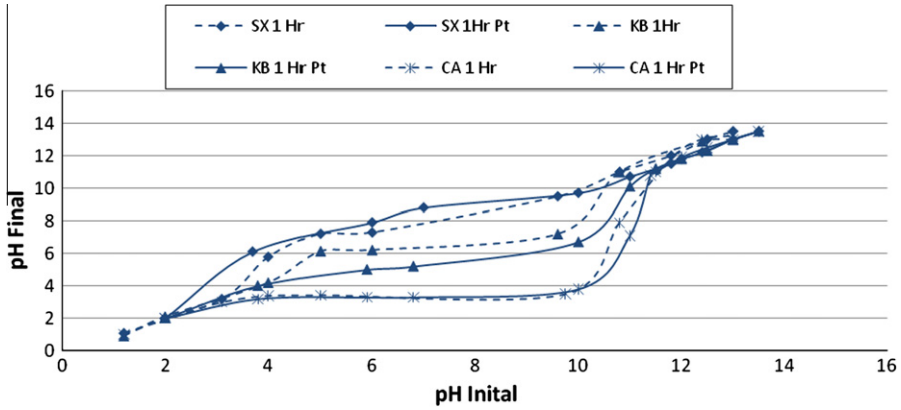

Fig. 8. Comparison of the pH shift with and without Pt tetraammine.

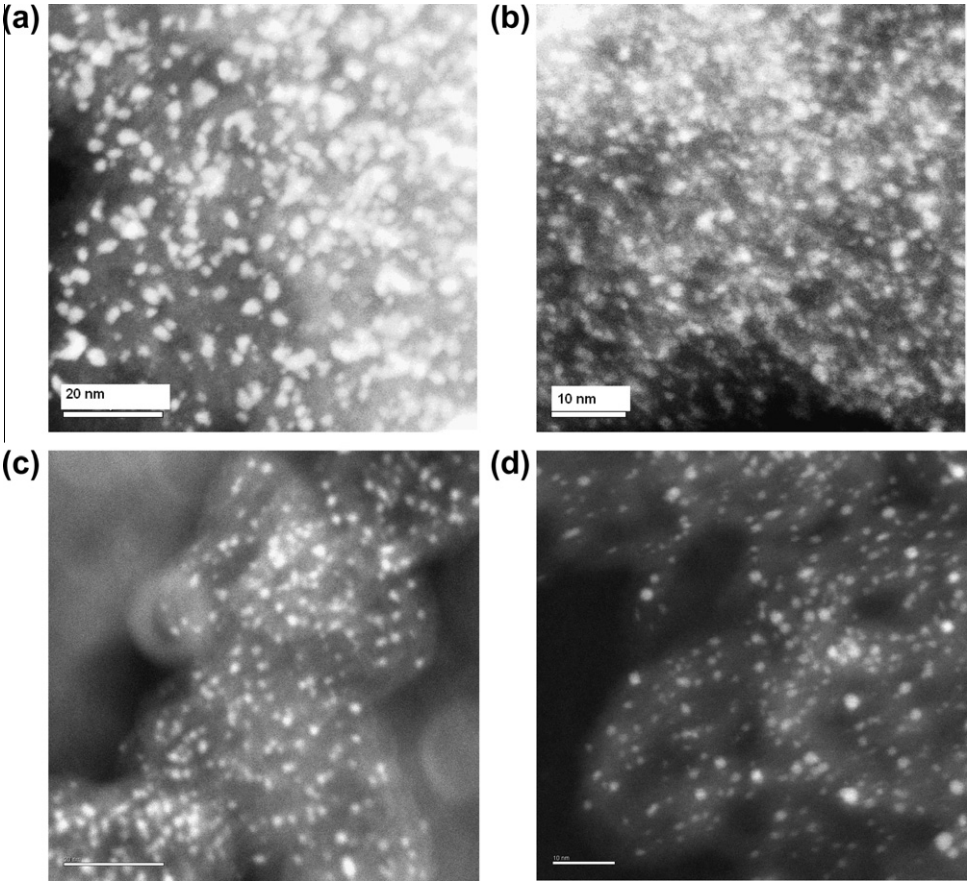

Fig. 9. STEM images of CPA on different carbon supports (a) SX-Ultra SEA, (b) SX-Ultra DI 13.5% Pt, (c) K300 SEA, and (d) K300 DI 17.9% Pt.

relatively narrow breadth of the pH uptake volcano plots of Fig. 4 relative to its width over alumina [4].

The pH plateau for the PZC 4 Timrex carbon (Fig. 3b), on the other hand, is as wide or wider than the same surface loading of a mesoporous silica, and the Timrex appears to adsorb protons below its PZC to a higher degree than does the silica. This suggests an amphoteric carbon surface with a density of proton exchanging groups that are on the order of those in silica. Correspondingly, the uptake volcanoes for PTA over the mid- and low-PZC carbons (Fig. 6b and c) are about as broad as those over silica [5]. Characterization of oxidized, low-PZC carbons of yields values in the range of 0.7–4.6 OH/nm^2 by titration [12,19,37,39] and 0.5–4.1 OH/nm^2 by CO and CO_2 desorption [12,19,37,39]. Hydroxyl densities in the neighborhood of 5 OH/nm^2 are typically cited for silica [3].

Third, significant differences between initial and final pH are observed at high surface loadings of both sets of carbon (Fig. 3a and b), where many syntheses in the literature are performed. There appears to be widespread neglect of the pH buffering effect of the carbon surface during metal adsorption, even while some groups have used "mass titration" [17] or the "pH slurry" [20,29,40] methods to find carbon PZC. In reporting adsorption

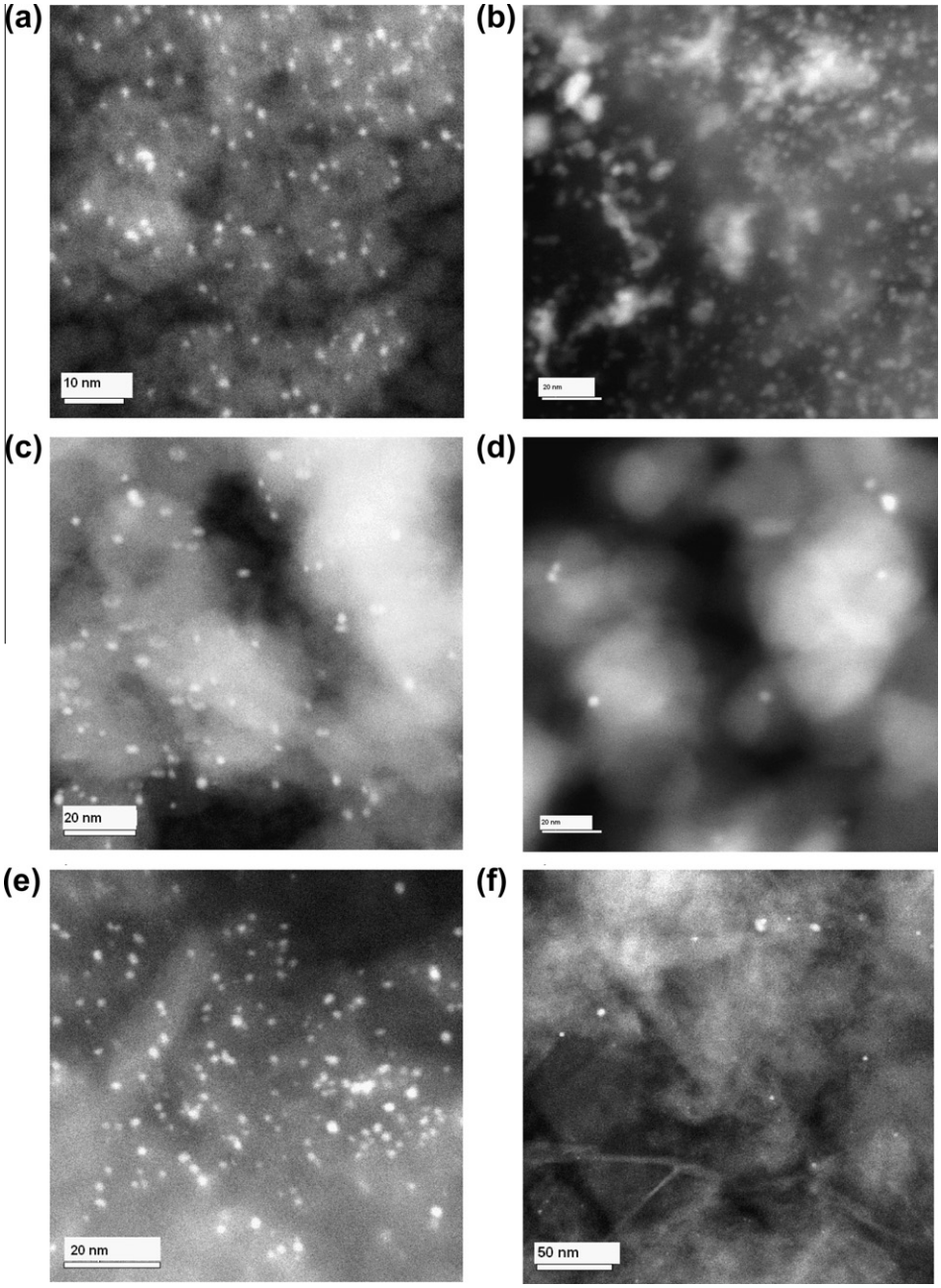

Fig. 10. STEM images of PTA on different carbon supports: (a) KB-B SEA, (b) KB-B DI, 5.3% Pt, (c) Printex U SEA, (d) Printex U DI, .52% Pt, (e) Timrex SEA, and (f) Timrex DI, 2.3% Pt.

data, the vast majority of studies report initial but not final pH values.

We suspect that in many published preparations, the buffering effect of the carbon is not overcome and surfaces are not strongly charged. A number of groups studying PTA adsorption over various types of oxidized carbon have employed a ratio of 1 g of carbon in 10 cm^3 of solution. For example, the group of Rodriguez-Reinoso et al. employed a carbon of 918 m^2/g [23] for a surface loading of 92,000 m^2/L and that of Coloma et al., 863 m^2/g [26] for 86,000 m^2/L. These surface loadings would cause pH buffering even more drastic than that seen in Fig. 3 and would require an initial pH near 13 to attain a final pH near the optimal value of 12 to strongly adsorb PTA. In neither of these studies [23,28] do we believe that electrostatic interactions were present, nor were the particles small (Table 3). The ramifications of surface charging during impregnation on final particle size will be fully discussed in a later section.

Verde et al. employed a 220 m^2/g oxidized carbon black (Vulcan XC72) at 22,000 m^2/L [24] and recorded the shift of pH from the initial value near 7 to about 4.4 as the carbon was contacted with the PTA solution (Fig. 4 in [24]). They correctly attributed this pH shift to acidification caused by the oxygen containing surface groups but, since no metal was adsorbed, assumed that this the surface was incapable of adsorbing metal ions which would have released even more protons via ion exchange. Inferring that the PZC of this carbon is about 4.4 from that experiment, and according to Fig. 6 above, significant metal uptake via electrostatic adsorption would indeed have occurred had the impregnating solution been sufficiently basified to achieve a final pH of 12.

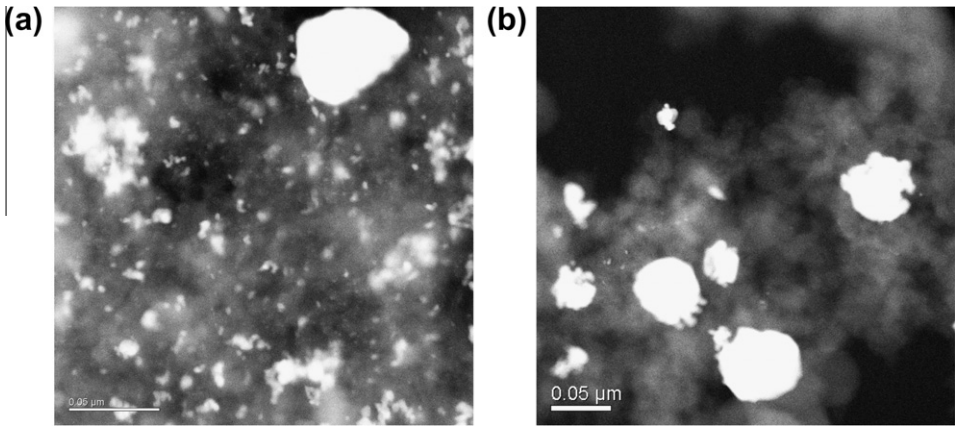

Fig. 11. Representative STEM images of materials prepared by DI with Pt(II) from sodium tetrachloroplatinate: (a) SXU 13.5 wt% and (b) Vul 10 wt%.

4.2. Adsorption at short contact time – electrostatic mechanism

Both Pt complexes in their respective pH ranges (anionic at low pH, cationic at high pH) and at the 1-h contact time qualitatively exhibit the features of electrostatic adsorption. The downturn in uptake at each pH extreme seen in Figs. 4 and 6 can be attributed to the decrease in adsorption equilibrium constants caused by high ionic strength [3]. This effect has been observed previously for a number of base metal anionic and cationic complexes adsorbing onto carbon [41]. The narrowness of the "volcano" shape at low pH may stem from the lower density of surface O groups on carbon relative to silica or alumina (Fig. 3). For both anion and cation adsorption, there exists an optimal pH at which the electrostatic interaction appears strongest. At 500 m^2/L for 180 ppm CPA over high-PZC carbons, this pH is about 2.9, while for 312 ppm PTA over mid- and low-PZC carbons at 2000 m^2/L, the optimal pH appears to be near 12. To our knowledge, this is the first report of an optimal pH at which to perform Pt anion and cation adsorption over carbons of high and low PZC, respectively. In our experience, the two pH optima are relatively insensitive to surface loading and metal concentration.

Given these features we believe that it is much more appropriate to consider the uptake of these Pt complexes onto carbon at short contact times as "electrostatic adsorption" and not "ion exchange" as cited by a number of groups [22,29,38,40]. The most intriguing claim of an ion exchange mechanism is proffered in the work of Amine et al. [38] who show a correlation of PTA uptake with carboxylic acid groups over a number of oxidized carbons (Denka Black, Vulcan XC72, and BP 2000). They observed a rapid decrease in solution pH from initial values around 6, likely the initial pH of PTA complex dissolved in deionized water, to final values of 3.8–2.6, with the more oxidized surfaces resulting in lower final pH. As mentioned above, they did not conduct control experiments in the absence of PTA to determine the pH shift that would have been induced by the carbon surface alone. We suspect the pH shifts would have been identical. The lowering of final pH they observed is consistent with the shifts expected with increasingly acidic PZC carbons. Also, they saw increases in the uptake of anionic Pt chlorides with increased oxygen content, which runs counter to an ion exchange mechanism.

In the Amine et al. work, significant Pt uptake was observed at these conditions, whereas in the present work, PTA solutions with initial pHs of 6 over mid- or low-PZC carbons that end up at pH 3 (Fig. 6c and e, and Fig. 7b and c) do not show any adsorption. The uptake of Pt observed by Amine et al. may result from the relatively high Pt concentration employed, 10,000 ppm PTA, versus the 200 ppm PTA used in the present work. The high concentration of Pt would have ensured that a significant amount of Pt would simply be imbibed by the support as it was contacted with the surface, although simple imbibition does not account for the increased uptake of PTA with increasing surface oxygen content. Curiously, increasing surface oxygen also led to increased uptake anionic CPA in that work [38] and yielded particles that were very large (>100 nm). Further complicating the comparison is that Amine et al. do not report the amount of carbon placed in contact with the high concentration PTA and CPA solutions; the surface loading of carbon and the fraction of Pt adsorbed are unknown for their system.

The Amine et al. results notwithstanding, an electrostatic mechanism appears especially appropriate for cationic Pt adsorption. In Figs. 6 and 7, there is little difference in uptake between one and 24 h. There is also no difference in pH from one to 24 h, and pH shifts in the presence and in the absence of PTA in solution (Fig. 8) are essentially the same. This is to say that proton transfer and adsorption equilibrate rapidly and independently. These are key aspects of the electrostatic adsorption mechanism [3]. The most significant discrepancy of the data in Fig. 6 from the electrostatic model is that the surface density is not as high as predicted for several of the carbons, in particular, the S51 and KB samples. These materials possess the highest surface areas and smallest pore size. It has been shown in a separate paper using a series of xerogel carbon materials with controlled micro and meso-pore size, that uptake of the tetraammine complex correlates nicely with mesoporous area [33], that is, the bulky platinum tetraammine complex that retains two hydration sheaths (a total hydrated diameter of 1.5 nm) is too large to enter into small micropores of high surface area carbons. The CPA complex, which retains only one hydration sheath, is apparently small enough to access even the smallest micropores as its surface density is as high as expected for all carbons.

4.3. Adsorption at long contact time – reductive mechanism

In the present set of data, a reductive adsorption mechanism is indicated for CPA at low pH by several features. The first indication is that adsorption equilibrium is not attained quickly; whereas almost no change in PTA uptake or pH shift is observed between 1 and 24 h (Figs. 6 and 7), and pH shifts are the same in the presence and the absence of PTA in solution (Fig. 8), Fig. 4 reveals significant uptake between one and 24 h, and Fig. 5 shows significant H^+ released into solution from CPA contacted for long times. It is notable that the narrow shape of the volcano plots is kept at long times; as the pH of a particular solution drops, the uptake of Pt increases,

Table 3
Summary of Pt/C preparation literature.

Ref.	Metal wt%	SA (m^2/g)	Meth.	Red. (K)	Disp. (%)	Size (nm)
CPA						
Activated carbon						
40	1	1457	IE	498	36	(2.7)
40	0.78	1095	IE	498	19	(5.2)
25	0.85	976	WI	623	33	(3.0)
25	0.86	920	WI	623	35	(2.9)
25	0.84	890	WI	623	38	(2.7)
23	1.1	659	IWI	673	21	5.7
23	0.91	918	IWI	673	41	2.6
44	1	1661	IWI	373, 623		
17	5.5	1141	IWI	673	42	(2.4)
17	5.5	1163	IWI	673	23	(4.3)
17	5.5	1128	IWI	673	11	(9.1)
17	5.5	1099	IWI	673	3	(33.0)
17	5.5	1437	IWI	673	10	(10.0)
21	1	1004	IWI	623	83	(1.2)
21	1	946	IWI	623	6.9	(14.5)
21	1	977	IWI	623	13.3	(7.5)
21	1	1065	IWI	623	15.9	(6.3)
21	1	976	IWI	623	33.6	(2.9)
21	1	876	IWI	623	31	(3.2)
21	1	890	IWI	623	38	(2.6)
21	1	1108	IWI	623	42.3	(2.4)
43	1	410	WI	523	84	1–3
43	1	1830	WI	523		1–3
43	1	1270	WI	523	57	1–3
43	1	1140	WI	523	52	1–3
43	1	610	WI	523	26	1–3
43	1	410	WI	523	84	1–3
24	1.7	220	WI	723	(50–25)	2–4
24	1.2	200	WI	723	(50–25)	2–4
24	1.3	200	WI	723	(50–25)	2–4
24	1.2	220	WI	723	(50–25)	2–4
Blacks						
16	1	300	IWI	623	(59)	1.7
16	1	325	IWI	623	(77)	1.3
27	0.93	956	IWI	623–773	(28)	3.6
27	0.94	917	IWI	623–774	(19)	5.1
27	0.96	918	IWI	623–775	(39)	2.6
27	1.07	895	IWI	623–776	(42)	2.4
29	0.98	580	IWI	623	80	(1.2)
29	0.96	730	IWI	623	15	(6.6)
29	0.92	830	IWI	623	20	(5.0)
29	0.78	530	IWI	623	70	(1.4)
29	0.9	990	IE	673	9	(11.1)
29	0.9	975	IE	673	14	(7.1)
38	68	257	WI	453		>100
38	70	1500	WI	453		>100
Xerogels						
42	1–4.5	645	WI	423	100–65	1–1.5
33	8–10		SEA	473	80–85	1.1–1.2
34	7.5–23	643	SEA	473	(53–50)	1.9–2.0
34	15	643	SEA	673	(50)	2.0
PTA						
Activated carbons						
40	1	1457	IE	498	34	(2.9)
40	0.69	1095	IE	498	18	(5.5)
23	1.32	918	IWI	673	8	13.5
23	0.68	918	IWI	673	12	9
23	0.68	918	IWI	673**	68	1.6
23	1.18	918	WI	673	8	13.5
23	1.26	918	WI	673	4	27.0
23	0.73	918	WI	673	5	21.6
23	0.73	918	WI	673**	19	5.7
28	1	863	WI	673**	20	5
28	1	910	WI	673**	9	12
Blacks						
29	0.62	580	IWI	623	70	(1.4)
29	0.96	730	IWI	623	28	(3.5)
29	1.05	830	IWI	623	40	(2.5)
29	0.91	530	IWI	623	20	(5.0)
22	0.4	990	IE	673	12	(8.3)
22	1	975	IE	673	5	(20.0)
24	0.07	200	WI	723	(100–33)	1–3
24	0.05	220	WI	723	(100–33)	1–3
38	21	257	WI	453	(83)	1.2
38	29	1500	WI	453	(100)	1
Xerogels						
33	1–5		SEA	473	75–85	1.2–1.3

** Heating in He at 673 K prior to reduction.

causing the mid-pH range points to "climb up the side of the volcano" at long contact times.

A number of groups have characterized the reduction of Pt from CPA during contact with carbon, using XPS and TPR [16,18,21,23,25,30,31]. In a later paper, we will present results on $[PtCl_6]^{2-}$ hydrolysis and on the reduction of Pt(IV) which occurs over carbon (but not over alumina) with EXAFS and XANES. It appears that Pt(IV) is necessary for this reaction to occur, as the Pt(II) chloride IWI preparations performed at the same initial pHs as the Pt(IV) preparations yielded very large, agglomerated particles that did not appear to interact with the surface (Fig. 11 and Table 2).

The chemical interaction is fundamentally different from an electrostatic mechanism in which the CPA complexes retain one hydration sheath and are above the surface as "outer-sphere" complexes. The chemical mechanism involves the close approach of the Pt complexes to the carbon surface as they react with the aromatic rings. In this interaction, the hydration sheath would be lost, allowing a higher density of complexes to adsorb. This can explain the higher adsorption density observed over carbon (up to about 2 μmol/m^2 at 24 h in Fig. 4) when compared to the normal maximum of 1.6 μmol/m^2 observed over alumina [4]. The newly formed hydroxyl groups can be protonated and might also adsorb Pt anions. The two mechanisms appear to act in parallel with the electrostatic mechanism predominating at short time scales on the order of minutes or tens of minutes and the chemical mechanism predominating at long contact times of hours or days.

The chemical mechanism mitigates the need to optimize the pH of CPA adsorption and explains the success of preparations utilizing CPA in which no attention has been paid to carbon buffering. In many cases, days or multiple days of contact are allowed [24,25,37]; as will be discussed in the next section, this mechanism appears to predominate at dry impregnation conditions.

4.4. Pt particle synthesis

Literature results for carbon-supported Pt catalysts prepared by traditional aqueous impregnation methods using CPA and PTA are summarized in Table 3. (A more general table including methods such as organic impregnations, microwave heating, and ultrasound dispersion and involving high metal loadings as would be required for electrocatalysts will be given in a later paper.) The three common methods in Table 3 are (1) incipient wetness impregnation, in which the amount of solution just needed to fill the pore volume of the support was employed and no adjustment of pH was made, (2) wet impregnation with an excess of solution and allowing it to evaporate while stirring, with no control of final pH, and (3) ion exchange in which basic pH values of the impregnation solutions are utilized in an attempt to elicit the exchange of protons from the surface carboxylic acid groups with Pt ammine cations. Strong electrostatic adsorption in which the metal complexes are adsorbed at the pH of strongest electrostatic attraction has been recently employed with both CPA [33,34] and PTA [33].

Except for the works of Lambert et al. [33] and Amine et al. [38,39], small particles were achieved with PTA using high surface area supports only at low metal loading and correspondingly low surface density; Verde et al. have produced 1–3 nm particles with wet impregnation at 0.05–0.07 wt% [24]. Roman-Martinez et al. [29] produced 1.4 and 2.5 nm particles with IWI on 580 and 830 m^2/g carbon black at 0.62 and 1.05 wt%, Fuente et al. [40] synthesized 2.9-nm particles at 1 wt% over a 1457 m^2/g black, and Rodriguez-Reinoso et al. [23] produced 1.6-nm particles at 0.68 wt% over a 918 m^2/g activated carbon support. In the latter work, a helium heat treatment is cited to dramatically reduce the particle size (from 9 to 1.6 nm for the 0.68 wt% sample); this treatment has been employed by others [28,30] with less success.

The larger size of many of the PTA preparations in Table 3 can be attributed to insufficiently basic conditions to cause significant deprotonation of the carbon support. In the IWI preparations, no adjustment of pH is made and the ratios of carbon to liquid employed typically result in surface loadings above 100,000 m^2/L. As mentioned in the section above, at this condition, the carbon surface is negligibly charged such that no metal precursor–surface interaction occurs. Even when "ion exchange" has been employed, the initial pHs employed are insufficiently basic to produce a strong surface charge. For example, an initial pH of 9 was employed in [40] with a surface loading of 110,000–150,000 m^2/L (1 g of 1095 or 1475 m^2/g carbon in 10 mL), an initial pH of 9.5 was employed with surface loadings of 86,000–91,000 [28,30], and an initial pH of 8.5 was employed in [22] with 1 g of 990 m^2/g carbon in 10 mL, or 100,000 m^2/L. Fig. 3 shows that an initial pH of about 13 is needed to arrive at the optimal final pH of 12 for such high surface loadings. Starting at an initial pH of 8.5–9.5, the final pH is most certainly at the PZC of the support. The relatively small amount of base initially added to the solutions was not able to induce a strong charge on the surface.

In contrast, the final pHs of SEA preparations are such that strong electrostatic interactions are ensured. The initial high dispersion of the strongly adsorbed precursor is maintained as the metal is reduced, with a simple reduction in hydrogen. SEA-prepared particles from PTA were small even at relatively high surface densities of Pt (Table 2). Small particles (2.0 nm) were achieved with PTA at 5.3 wt% over the high surface area activated carbon (KB, 1500 m^2/g) and 1.3-nm particles at 4.5% over a 660 m^2/g carbon xerogel [33]. In every case, the SEA-prepared materials have a smaller particle size and narrower particle size distribution than the corresponding IWI-prepared samples. As mentioned in the results, higher temperature ramp rates caused sintering of particles but the higher reduction temperature of 400 °C (instead of 200 °C) comparable to most literature reports did not.

The main limitation of SEA with mid- and low-PZC carbons is pore exclusion in high surface area materials. This limitation has been overcome by employing high surface area mesoporous xerogel carbons [34]. The SEA limit for Pt tetraammine adsorption, assuming no pore exclusion, is about 0.84 μmol/m^2 [32]. If higher loadings than this are desired, the SEA procedure can be repeated after reduction of the first adsorbed monolayer, with no increase in particle size. In this way, a 23 wt% Pt sample from three successive SEA procedures with Pt anions was obtained over a 643 m^2/g carbon xerogel [34]. It appears that as the monolayer of precursors densifies into metal particles during reduction, the majority of the carbon surface is uncovered and behaves essentially the same as prior to the adsorption/reduction cycle. The same procedure could be performed with Pt cations over low- to mid-PZC carbons.

Another limitation with SEA of PTA complexes is that it cannot be administered with high-PZC carbons, which do not adsorb PTA strongly (Fig. 6a and b). This can be overcome by oxidizing the support, of course, which lowers the support PZC and allows full uptake of PTA [33].

The PTA synthesis of Amine et al. [38] is striking in that very small particles (0.7–1.7 nm) were achieved at very high surface densities (21 wt% Pt over a 257 m^2/g Vulcan XC 72 and 29 wt% over 1500 m^2/g BP2000). The disadvantages of this method would appear to stem from the handling and recycling of the 10,000 ppm PTA solutions employed, which presumably are not depleted of Pt during the synthesis process. In SEA with low metal concentrations at the optimal pH, virtually 100% of the metal is adsorbed by the support.

In the CPA preparations of Table 3, incipient wetness impregnation is the most common procedure. Several groups have employed wet impregnation [22,42] and two have referred to the contacting as ion exchange [22,40]. In general, it appears that small Pt particles can be produced at low metal loadings over high surface area supports more readily with CPA than with PTA as particle sizes 3 nm or below are commonly seen at low Pt loadings.

In Table 2 and in Refs. [33,34], it is seen that SEA preparations at the optimal pH yield particles that are as small as or smaller (1.1–2.8 nm) than those reported in the literature, even at the higher metal loadings employed in these studies. Thus via SEA, a 28 wt% Pt loading was achieved on BP2000 black in a single adsorption step, and the reduction yielded 2.0-nm particles with a tight particle size distribution. A comprehensive study of high surface area carbons and high Pt loadings via SEA and DI will be presented in a later paper.

While we employed a reduction temperature of 160 °C for CPA, determined by TPR and XPS to be the minimum temperature needed to reduce the Pt(IV) to Pt metal, and which is substantially below the reduction temperature employed by most others in Table 3, it was determined in a previous work [34] that a higher reduction temperature of 450 °C did not significantly increase the particle size for a 15 wt% catalyst.

Surprisingly, the DI preparations with CPA (Fig. 9 and Table 2) yield particles that are on average as small and have size distributions as narrow as the SEA counterparts. This may arise in part because the acidity of the CPA significantly protonates the carbon surface. For a previous WI preparation [33], for example, the initial pH and final pH were 1.9, which is not too far from the optimal pH. However, the initial pHs of the various DI preparations are quite acidic. For example, for 10–28 wt% Pt over 250–1475 m^2/g carbons with pore volumes of 1–2 mL/g used for DI, the initial pH values of the CPA solutions are typically below 0. There is little or no pH buffering at these strongly acidic conditions (Fig. 3a) even at incipient wetness, and so the final pH will be very far below the optimal value, in the regime in which adsorption tapers off dramatically (Fig. 4). In fact, the Pt(II) chloride solutions were pH-adjusted to the same low values as the corresponding CPA preparations and resulted in very large particles. It can be hypothesized, therefore, that the reduction reaction shown in the earlier equation plays a significant role in the establishment of well-dispersed Pt precursors during dry impregnation and during SEA at long contact times as well. It might also be conjectured that this reaction is more prevalent at higher Pt surface densities, as the particle sizes shown in Table 2 are for the relatively high Pt densities corresponding to a monolayer of hydrated CPA complexes. From the literature, it appears that particles sizes are larger when lower Pt loadings (and lower Pt surface densities) are employed. Work is ongoing to confirm this trend of decreasing Pt particle size with increasing Pt content using DI.

The catalytic activity of SEA-prepared Pt/carbon catalysts is very high for benzene hydrogenation [33] as well as cathode fuel cell reactions [34]. The residual chloride in the CPA preparations which leads to lower activity via poisoning can be removed by high-temperature calcinations [34]. For benzene hydrogenation, the highest activity stems from a PTA preparation on a high surface area, xerogel carbon that yields highly loaded, well-dispersed Pt on a diffusion-free mesoporous carbon support [33].

5. Conclusions

Strong electrostatic adsorption of Pt onto carbon can be used with CPA at low pH and PTA at high pH to achieve a monolayer or submonolayers of Pt precursors that retain their high dispersion with a simple reduction in hydrogen.

The interaction of platinum tetraammine with mid- or low-PZC carbon surfaces at high pH appears to be wholly electrostatic in nature; the SEA method of preparation consistently gives smaller particles sizes with narrower particle size distributions than DI preparations for which no precursor–support interaction occurs. In most previous studies, the buffering of the solution pH by the carbon surface has not been adequately accounted for and electrostatic adsorption has not been achieved with PTA; this is probably the main reason why the electrostatic adsorption mechanism outlined by Radovic and Rodriguez-Reinoso [14] for carbon has not been universally recognized to date. The optimal final pH of PTA impregnation is close to 12 for a wide number of carbons.

Preparation with PTA avoids the problem of residual chloride which can hinder activity for certain reactions. One drawback to PTA preparations is the exclusion of the large precursor complex, which retains two hydration sheaths, from a significant fraction of the pore volume of microporous carbons. This can be counteracted by utilizing mesoporous carbon. PTA will also not adsorb to a significant extent over high-PZC carbons; this can be solved by lowering the PZC of the carbon by surface oxidation. In this fashion, highly loaded catalysts (20 wt% Pt or more) can be synthesized with particle sizes of 1–2 nm and narrow size distributions.

The interaction of CPA with high, mid-, or even low-PZC carbon surfaces at low pH is comprised of an electrostatic component at short contact times and a reactive component at longer contact times. The reactive component involves the reduction of Pt(IV) and the oxidation of the carbon surface and mitigates the need to adsorb CPA at the pH of strongest electrostatic interaction. While SEA preparations at the optimal final pH of about 2.9 consistently yield Pt particles with small size (1.1–2.8 nm) and narrow size distributions, simple DI preparations with CPA yield a similar range of particle size and size distribution, at least when the metal loading is high. It is believed that the adsorptive reduction reaction plays a significant role in the dispersion of the CPA precursor during dry impregnation.

Acknowledgment

The support of the former CTS division of the Engineering Directorate of the National Science Foundation is gratefully acknowledged.

References

[1] J.R. Regalbuto, in: J.R. Regalbuto (Ed.), Catalyst Preparation, Science and Engineering, Taylor & Francis, 2007.
[2] J.R. Regalbuto, in: K.P. de Jong (Ed.), Synthesis of Solid Catalysts, Wiley-VCH Verlag, 2009.
[3] X. Hao, W. Spieker, J.R. Regalbuto, J. Colloid Interface Sci. 267 (2003).
[4] J.R. Regalbuto, A. Navada, S. Shadid, M.L. Bricker, Q. Chen, J. Catal. 184 (1999) 335–348.
[5] M. Schreier, J.R. Regalbuto, J. Catal. 225 (2004) 190–202.
[6] J.T. Miller, M. Schreier, A.J. Kropf, J.R. Regalbuto, J. Catal. 225 (2004).
[7] L. Jiao, J.R. Regalbuto, J. Catal. 260 (2008) 329–341.
[8] L. Jiao, J.R. Regalbuto, J. Catal. 260 (2008) 342–350.
[9] M. Schreier, S. Teren, L. Belcher, J.R. Regalbuto, J.T. Miller, Nanotechnology 16 (2005) S582–S591.
[10] G.W. Huber, S. Iborra, A. Corma, Chem. Rev. 106 (2006) 4044–4098.
[11] D.A. Simonetti, J.A. Dumesic, Catal. Rev. Sci. Eng. 51 (2009) 441–484.
[12] J.M. Solar, C.A. Leon y Leon, K. Osseo-Asare, L.R. Radovic, Carbon 28 (1990) 369–375.
[13] C.A. Leon y Leon, J.M. Solar, V. Calemma, L.R. Radovic, Carbon 30 (1992) 797–811.
[14] L.R. Radovic, F. Rodriguez-Reinoso, Chem. Phys. Carbon 25 (1997) 243–358.
[15] X. Hao, L. Quach, J. Korah, W.A. Spieker, J.R. Regalbuto, J. Mol, Catal. A: Chem. 219 (2004) 97–107.
[16] F. Coloma, A. Sepulveda-Escribano, J.L.G. Fierro, F. Rodriguez-Reinoso, Langmuir 10 (1994) 750–755.
[17] M.A. Fraga, E. Jordao, M.J. Mendes, M.M.A. Freitas, J.L. Faria, J.L. Figueiredo, J. Catal. 209 (2002) 355–364.
[18] H.E. van Dam, H. van Bekkum, J. Catal. 131 (1991) 335–349.
[19] R.L. Jia, C.Y. Wang, S.M. Wang, J. Mater. Sci. 41 (2006) 6881–6888.
[20] F. Coloma, A. Sepulveda-Escribano, F. Rodriguez-Reinoso, J. Catal. 154 (1995) 299–305.
[21] G.C. Torres, E.L. Jablonski, G.T. Baronetti, A.A. Castro, S.R.d. Miguel, O.A. Scelza, M.D. Blanco, M.A.P. Jim6nez, J.L.G. Fierro, Appl. Catal. A: Gen. 161 (1997) 213–226.
[22] A. Sepulveda-Escribano, F. Coloma, F. Rodriguez-Reinoso, Appl. Catal. A: Gen. 173 (1998) 247–257.
[23] F. Rodrigez-Reinoso, I. Rodriguez-Ramos, C. Moreno-Castilla, A. Guerrero-Ruiz, J.D. Lopez-Gonzalez, J. Catal. 99 (1986) 171–183.
[24] Y. Verde, G. Alonso, R.V.H. Zhang, A.J. Jacobson, A. Keer, Appl. Catal. A: Gen. 277 (2004) 201–207.
[25] S.R. de Miguel, O.A. Scelza, M.C. Roman-Martinez, C. Salinas-Martinez de Lecea, D. Cazorla-Amoros, A. Linares-Solano, Appl. Catal. A: Gen. 170 (1998) 97–103.
[26] H. Kim, P. Kim, J.B. Joo, W. Kim, I.K. Song, J. Yi, J. Power Sour. 157 (2006) 196–200.
[27] C. Prado-Burguete, A. Linares-Solano, F. Rodriguez-Reinoso, C. Salinas-Martinez de Lecea, J. Catal. 115 (1989) 98–106.
[28] F. Coloma, A. Sepulveda-Escribano, J.L.G. Fierro, F. Rodriguez-Reinoso, Appl. Catal. A: Gen. 150 (1997) 165–183.
[29] M.C. Roman-Martinez, D. Cazorla-Amoros, A. Linares-Solano, C.S.-M.d. Lecea, H. Yamashita, M. Anpo, Carbon 33 (1995) 3–13.
[30] F. Coloma, A. Sepulveda-Escribano, J.L.G. Fierro, F. Rodriguez-Reinoso, Appl. Catal. A: Gen. 136 (1996) 231–248.
[31] R.W. Fu, H.M. Zeng, Y. Lu, S.Y. Lai, W.H. Chan, C.F. Ng, Carbon 33 (1995) 657–661.
[32] N. Santhanam, T.A. Conforti, W. Spieker, J.R. Regalbuto, Catal. Today 21 (1994) 141–156.
[33] S. Lambert, N. Job, L. D'Souza, M.F.R. Pereira, R. Pirard, B. Heinrichs, J.L. Figueiredo, J.-P. Pirard, J.R. Regalbuto, J. Catal. 261 (2009) 23–33.
[34] N. Job, S. Lambert, M. Chatenet, C.J. Gommes, F. Maillard, S. Berthon-Fabry, J.R. Regalbuto, J.-P. Pirard, Catal. Today 150 (2010) 119–127.
[35] J. Park, J.R. Regalbuto, J. Colloid Interface Sci. 175 (1995) 239–252.
[36] X. Hao, Ph.D. Thesis, On the Science of Catalyst Preparation: Platinum Impregnation Over Carbon, University of Illinois at Chicago, 2004.
[37] K.T. Kim, J.S. Chung, K.H. Lee, Y.G. Kim, S.J.Y., Carbon 30, 1992, pp. 467–475.
[38] K. Amine, M. Mizuhata, K. Oguro, H. Takenaka, J. Chem. Soc. Faraday Trans. 91 (1995) 4451–4458.
[39] K. Amine, K. Yasuda, H. Takenaka, Ann. Chim. Sci. Mater. 23 (1998) 331–335.
[40] A.M. Fuente, G. Pulgar, F. González, C. Pesquera, C. Blanco, Appl. Catal. A: Gen. 208 (2001) 35–46.
[41] V. Lopez-Ramon, C. Moreno-Castillo, J. Rivera-Utrilla, L.R. Radovic, Carbon 41 (2002) 2020–2025.
[42] N. Job, M.F.R. Pereira, S. Lambert, A. Cabiac, G. Delahay, J.-F. Colomer, J. Marien, J.L. Figueiredo, J.-P. Pirard, J. Catal. 2 (2006) 160–171.
[43] L.B. Okhlopkova, A.S. Lisitsyn, V.A. Likholobov, M. Gurrath, H.P. Boehm, Appl. Catal. A: Gen. 204 (2000) 229–240.
[44] S.R. de Miguel, J.I. Vilella, E.L. Jablonski, O.A. Scelza, C. Salinas-Martinez de Lecea, A. Linares-Solano, Appl. Catal. A: Gen. 232 (2002) 237–246.